Eccentric Taylor-Couette Flow with orbital motion of the inner cylinder

Andreas CHRISTL [1,*], Nicoleta HERZOG [1], Christoph EGBERS [1]

* Corresponding author: Tel.: ++49-0355-69-5015; Email: Andreas.Christl@TU-Cottbus.De
1 Dept. of Aerodynamics and Fluid Mechanics, Brandenburg University of Technology Cottbus, Germany
Keywords: Journal bearing, Lubricant Film, Eccentric Taylor-Couette Flow

Abstract: The flow in a Taylor- Couette system is one of the most explored flows today. The behaviour of the flow is characterized by Reynolds number, radii and aspect ratio. By reducing the gap width the Taylor-Couette system can be used as a simplified bearing model which has one additional feature. To cover flow effects of a real bearing the rotating inner cylinder moves on an offset track. Thus the system is also characterized by a varying annulus. That changes the eccentricity which is also related to the critical Reynolds number for the system. There is a higher Reynolds number for a higher eccentricity. This is used as a benchmark to validate the code. Depending on the eccentric position of the rotating inner cylinder one can notice either Taylor Vortex flow or Couette Flow.
After testing the code the gap width will be adjusted to realistic bearing geometries. This second part refers to bearing simulations where the gap width is adjusted to real bearing conditions. In Fact the present system is a simplified bearing, which covers not all details of a real one. It becomes more complex in later stages of the project, where oil feedings and notches are implemented as well as the occurrence of cavitation. Furthermore the offset tracks will be much more complex. The final goal is to develop a 3D simulation tool for hydrodynamic journal bearings that resolves effects like cross flow from the oil feedings and also cavitation. Known methods based on the Reynolds equations fail to predict important flow characteristics in complex bearing geometries due to their two dimensional nature. If sufficiently low local pressure areas occur, cavitation- related damages may appear. So the pressure distribution of the flow is of interest.

Keywords: Eccentric Taylor-Couette Flow, Journal Bearing, lubricant film

1. Introduction

The simplified Journal bearing can be considered as an eccentric Taylor-Couette System. The rotation of the inner cylinder leads to a high pressure region in the narrowed gap and a low pressure area in the expanding gap (*FIG.1*). High rotation rates induce small eccentricities due to the pressure in the gap. (*FIG.2*)

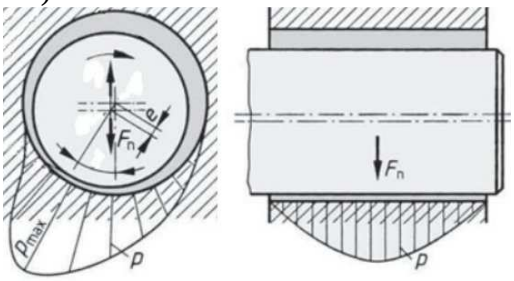

FIG.1: Pressure distribution in the gap. Left: cylindrical sectional view [5]. *Right: axial sectional view* [5]

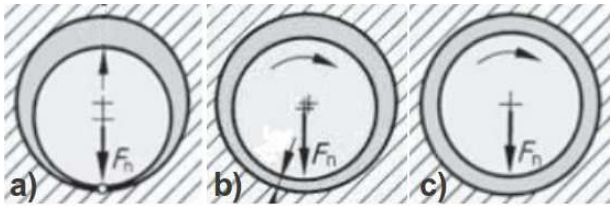

FIG.2: Analogy of Rotation rate and eccentricity of a bearing:
a) No rotation. b) Clockwise rotation of the inner cylinder, smallest gap shifted to the left. c) Very high rotation rate. The eccentricity is assumed to be 0 [5].

The next step from the Taylor- Couette System to the simplified bearing system is to implement a crankshaft offset track. These offset tracks are quite different for every engine. *FIG.3* shows the different types of bearings in and *FIG.4* two realistic offset tracks.

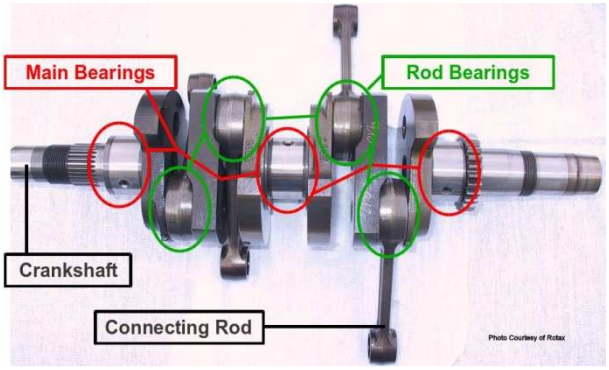

FIG.3: Main and Rod Bearings [13]

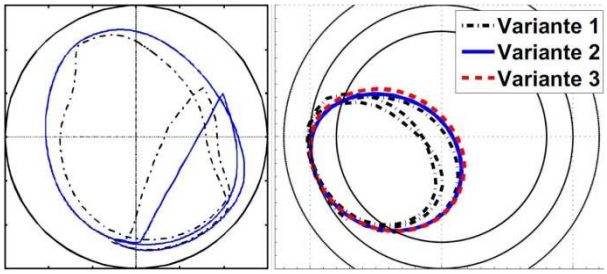

FIG.4: Real offset tracks [1], [4]

In this Work two types of simplified offset tracks were used. One track leads to constant eccentricity. The start position is eccentric. Then the anticlockwise rotating cylinder starts his clockwise orbit with a given radius for constant eccentricity (*FIG.5* middle). The other track causes oscillating eccentricity during one orbit. Here the start position is concentric. Then the shaft moves on an orbit too. At the half of the orbit the eccentricity is largest (*FIG.5* right). Both orbital movements are uniform. The last mentioned offset track will be used as a benchmark for the simulation code. The normalized gap width or clearance $\Psi=H_0/R_1$ is defined by the gap H_0, the difference of outer and inner cylinder normalized in respect to the inner cylinder. The normalized gap width 0.1 for the benchmark is much too large for a typical bearing clearance. It was chosen to reduce the numerical effort. Small gaps need a very extensive mesh resolution due to the large aspect ratio. Moreover, the critical Reynolds number for Taylor vortex flow is very high (*FIG.7*). A realistic clearances of $\Psi=0.001=1‰$ is presented in chapter 4. In these simulations scales and dimensions changes a lot. The most impressive one is the aspect ratio Γ, the ratio of the height and the gap width. $\Gamma=20$ was chosen for the benchmark with $\Psi=0.1$. For $\Psi=1‰$, $\Gamma=741$ was needed to fulfil the geometric inputs of the given bearing. So it is much more expensive to resolve the computation domain.

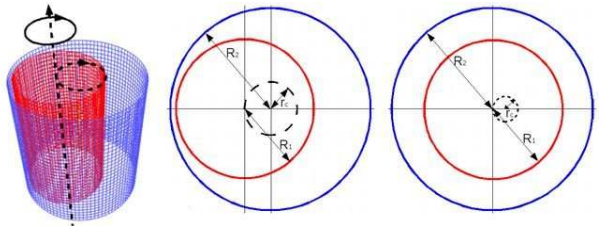

FIG.5: Simplified Offset Tracks: The 3D-Model (left). Orbit with constant eccentricity (mid) and Orbit with oscillating eccentricity (right).

2. Numerical Simulations

An incompressible finite-volume code was used to solve the Navier- Stokes Equation (1) on a moving mesh. For detailed information see [14], [3], and [6]. In this first stage of the project the fluid is considered to be Newtonian and isothermal. In general the lubricant in the bearing is non-Newtonian. A comparison with experiments from IEM i.G. Zwickau [14], [3], and [6] was drawn. In these experiments WACKER® AK 50 silicone fluid was used. This Fluid is assumed to be Newtonian.

$$\nabla \cdot U = 0\,,$$

$$\frac{\partial U}{\partial t} + (U \cdot \nabla)U = -\nabla \frac{p}{\rho} + \nu \nabla^2 U \qquad (1)$$

The boundary conditions are:
Fixed endplates: $\nabla p=0$; $U=0$. (Benchmark)
Open ends: $p=\text{const.}$; $\nabla U=0$.
Inner cylinder: $\nabla p=0$; $U=f \cdot Re$, $f=\text{const.}$
Outer cylinder: $\nabla p=0$; $U=0$.

3. Benchmark

The concentric rotating inner cylinder was set to an overcritical Reynolds number. Thus, the flow develops Taylor Vortices (TV). After this initial period the orbit was started. So the eccentricity increases and shows its maximum value after half of the orbit. If the eccentricity rises, the inner cylinder has to rotate faster to generate TV. For larger

eccentricities the slope of Re(ε) increases stronger (*FIG.6)*. Goal of this benchmark is to find the onset and decay of TV during one orbit. The inner cylinder rotates anticlockwise and the orbit was chosen to move in clockwise direction.

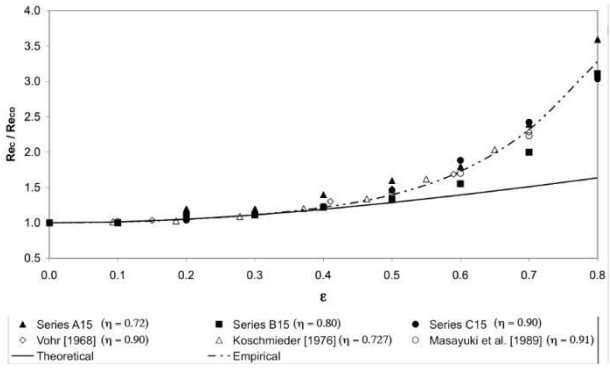

FIG.6: Critical Reynolds number Re for TV and corresponding Eccentricities [9].*The vertical axis shows the ratio of the critical Re for the eccentric position and the Re for the concentric position. The Linear theory only fits for small eccentricities. There is a raising slope in Re(ε) for higher eccentricities.*

The Parameters of the Simulations are:

Designation	Shortcut	Value	Unit
Radius of Inner Cylinder	R_1	1	m
Radius of Outer Cylinder	R_2	1.1	m
Radius Ratio	$\eta = R_1/R_2$	0.91	m
Gap Width	$H_0 = R_2 - R_1$	0.1	m
Normalized Gap Width	$\Psi = H_0/R_1$	0.1	
Height of Cylinders	B	2	m
Aspect Ratio	$\Gamma = B/H_0$	20	
Shift from concentric Position	e	0.075	m
Eccentricity	ε	0 - 0.75	
Cycle Duration	T_O	5; 25; 45	s
Radius of Orbit	R_O	0.0375	m
Tangential Velocity Inner Cylinder	U_T	1	m/s
Kinematic Viscosity	ν	0.0004	m^2/s
Reynolds number	$Re = H_0 \cdot U_T / \nu$	250	
Viscous Timescale	$\tau = (H_0)^2/\nu$	25	s

Tab.1: benchmark Parameter- onset and decay of TVF

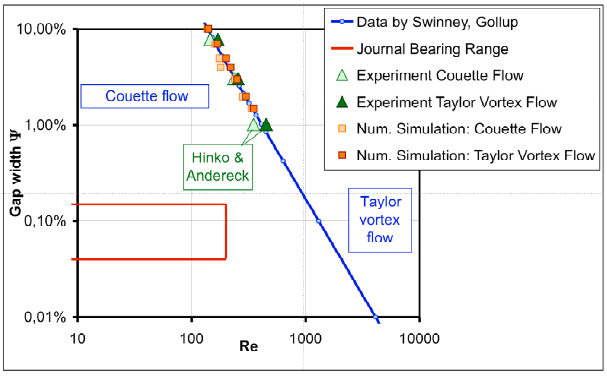

FIG.7: Typically clearances and Re for journal bearings [11]. *The clearance is given in %. 0.1% corresponds to Ψ=0.0001. The benchmark clearance is 10%.*

The pictures *(FIG.8), (FIG.9), (FIG.10)* show the magnitude of velocity at 10 post processing positions which can be found at the left of every picture. The rectangle plot on the right is an unwounded intermediate gap plane between inner and outer cylinder to overview the whole cylindrically plane. A red coloured maximum in the magnitude indicates a pair of counter-rotating TV. The first simulation *(FIG.8)* has a cycle duration of T=5s. Because of the time between onset and decay is too short there is no complete evolution of TV. The second simulation *(FIG.9)* has a cycle duration of T=25s which corresponds to one viscous time scale. The TV are quite well minted. The third *(FIG.10)* has T=45s. Here one can find full developed TV.

3.1. Orbit with T=5 s

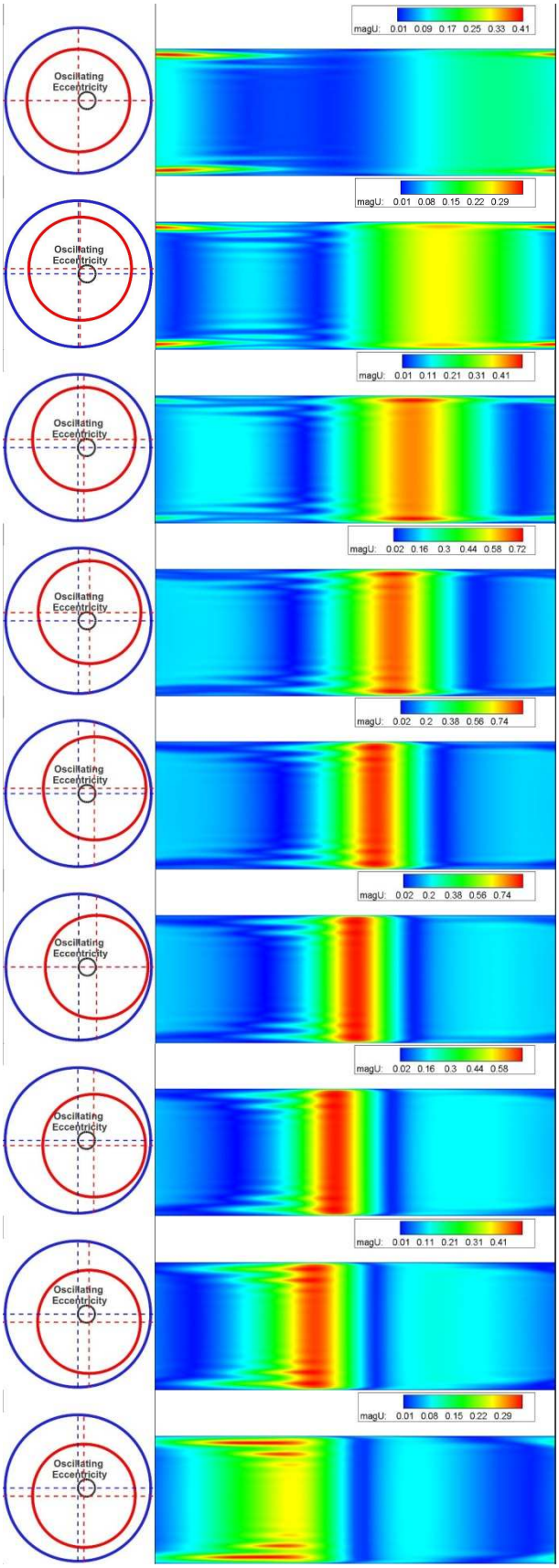

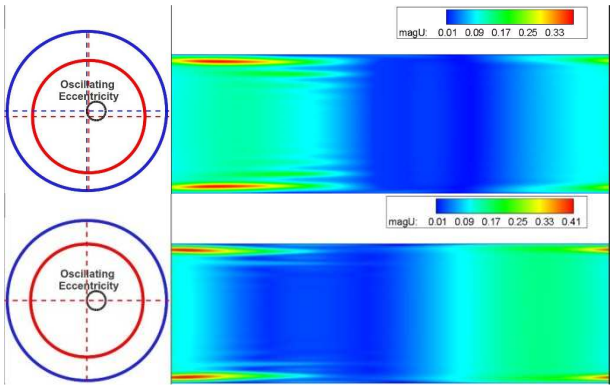

FIG.8: TV did not develop along the whole cylinder because the orbit is too fast. T=5 seconds. Re=250. There are just Ekman vortices near the end walls

3.2. Orbit with T=25 s

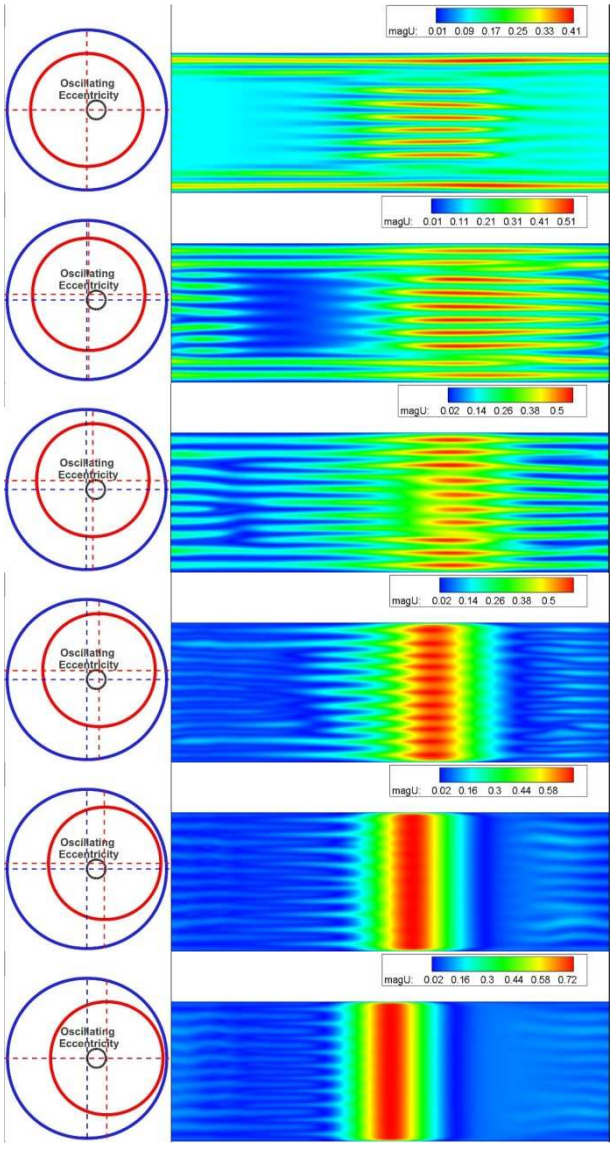

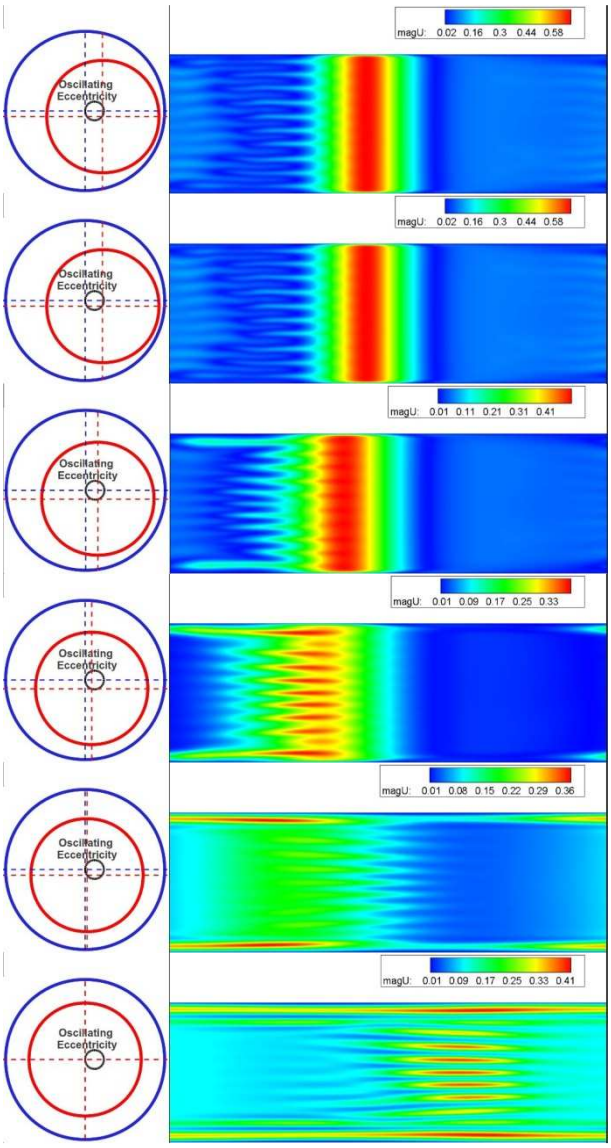

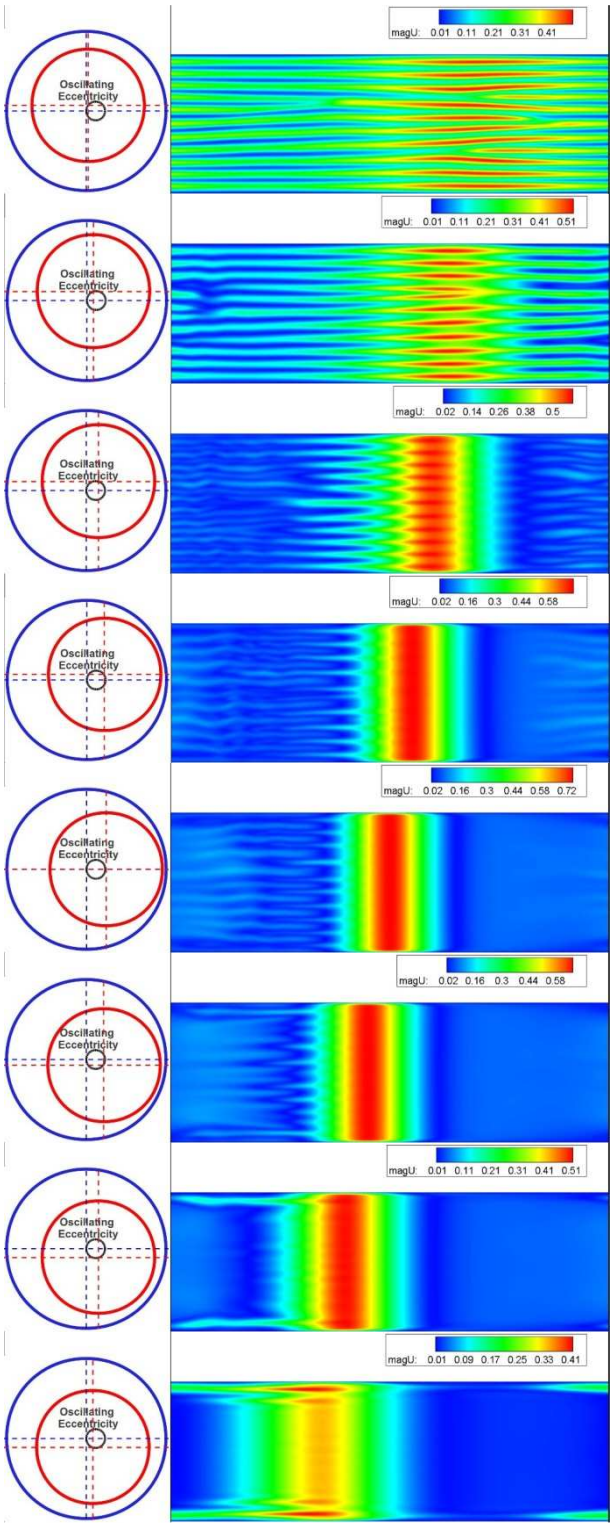

FIG.9: T=25 s. Re=250. Onset and Decay of TV during one orbit of viscous timescale. There are quite good developed TV for the corresponding positions (nearly concentric). Furthermore there exist different numbers of vortices (20, 22, and 24) in the flow. In the smaller gap smaller vortices begin to appear. During the orbit the gap will become locally larger, so the larger vortices and the aspect ratio does not fit together and adjust to a lower number of larger vortices.

3.3. Orbit with T=45 s

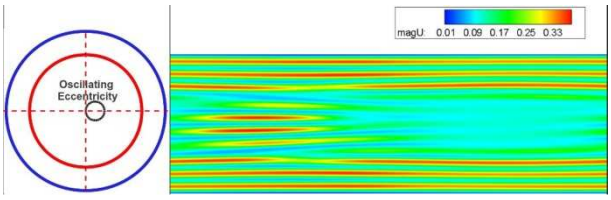

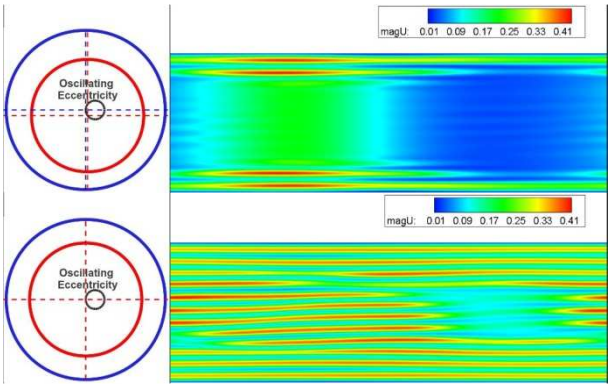

FIG.10: T=45 seconds. Re=250. TV develops along the whole gap in circumferential direction if the position is nearly concentric. The flow has enough time to shape the TV or to decay.

4. Numerical Simulation of realistic bearing geometries

After testing the code the gap width will now be adjusted to realistic bearing geometries. In the benchmark simulations the cycle duration was chosen in respect to the viscous time scale τ. Now there is a consequent time T for the offset track if the rotation rate is given. The time of one revolution of the crankshaft correlates with the cycle duration in the model. The inner cylinder radius R_1 is 99.9 % of R_2. So we have a clearance of 0.1 % or 1 ‰. The radius ratio ($\eta=R_1/R_2$) is approximately 0.9991.
In case of orbit with constant eccentricity the radius R_0 for the circular offset track is approximately $R_0=3.75\cdot10^{-5}$ m. In case of oscillating eccentricity $R_0=1.87\cdot10^{-5}$ m. This radius R_0 depends on the chosen eccentricity of the system. The eccentricity for orbit with constant eccentricity is set to $\varepsilon=0.75$. In case of oscillating eccentricity the maximum is set to $\varepsilon=0.75$. In both cases the crankshaft rotates with 4000 rpm. This leads to a cycle duration of T=0.015s, a tangential velocity of the inner cylinder of approximately 21m/s and a Reynolds number of Re=131.

Designation	Shortcut	Value	Unit
Radius of Inner Cylinder	R_1	49.95	mm
Radius of Outer Cylinder	R_2	50	mm
Radius Ratio	$\eta= R_1/R_2$	0.999	-
Gap Width	$H_0= R_2–R_1$	0,04995	mm
Normalized Gap Width	$\Psi= H_0/R_1$	0.001	-
Height of Cylinders	B	37	mm
Aspect Ratio	$\Gamma=B/H_0$	741	-
Tangential Velocity Inner Cylinder	U_T	20.923	m/s
Kinematic Viscosity	ν	$7.985\cdot10^{-6}$	m²/s
Reynolds number	$Re=H_0\cdot U_T/\nu$	131	
Viscous Timescale	$\tau= (H_0)^2/\nu$	$3.12\cdot10^{-4}$	s

Tab.2: Parameters of the small gap Ψ=1‰

4.1. Orbit with constant eccentricity

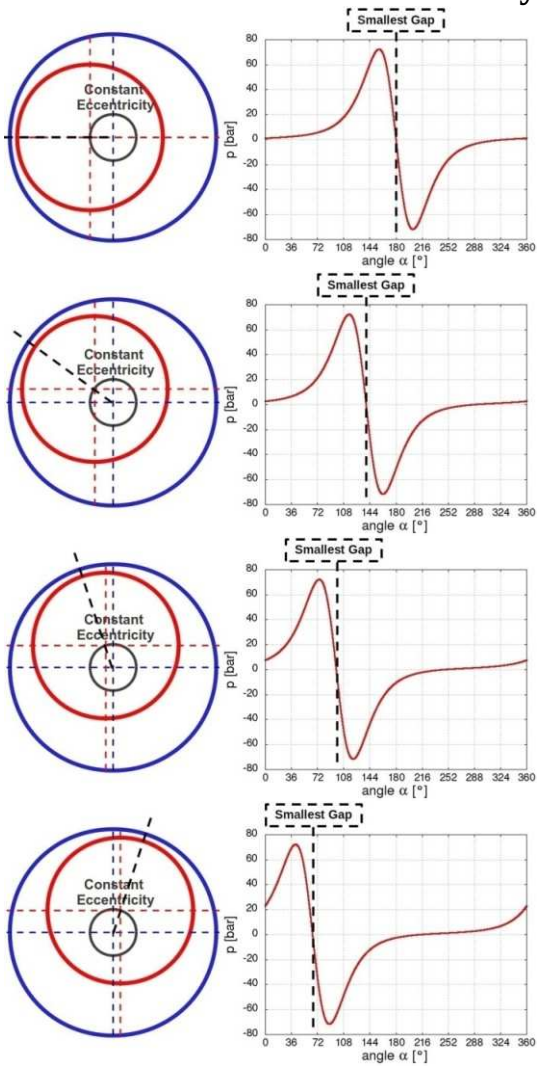

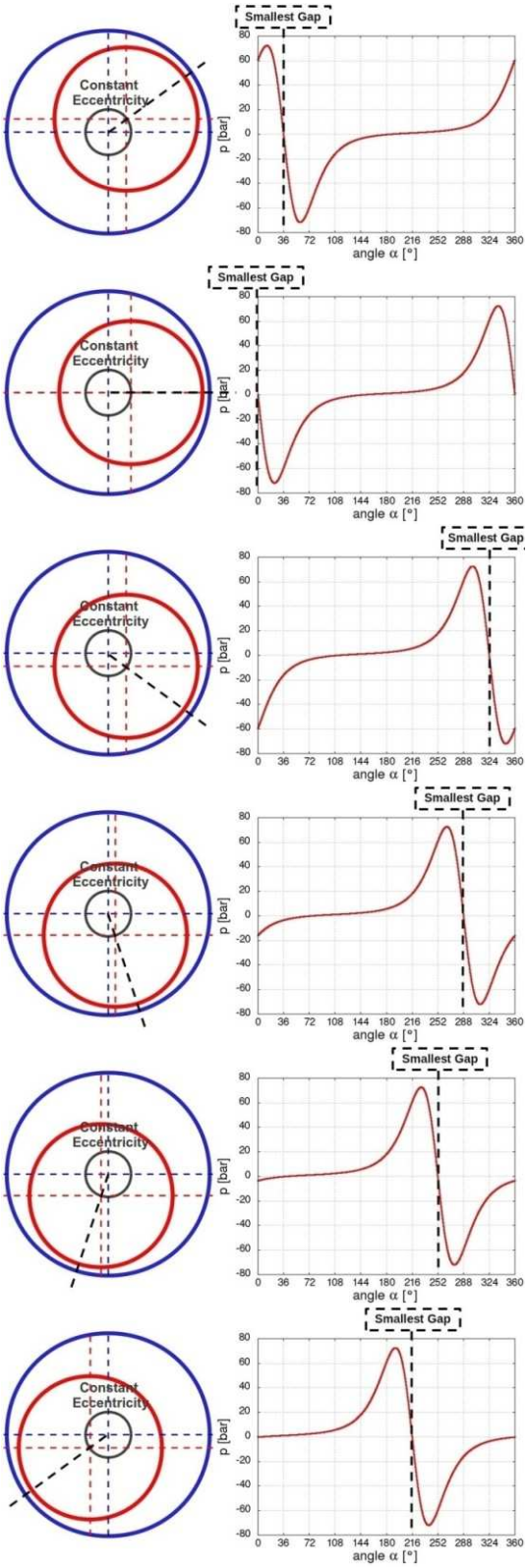

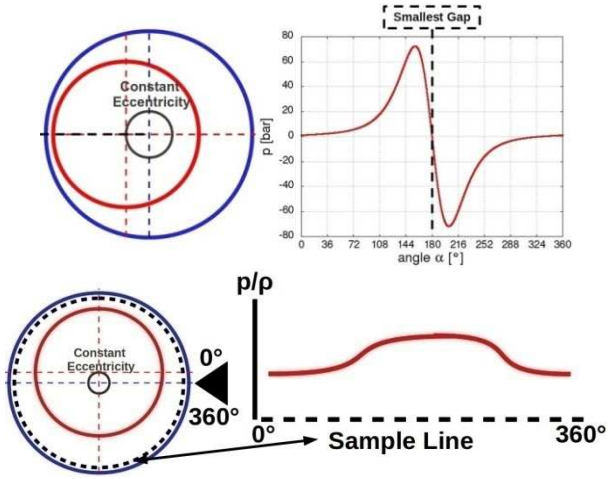

FIG.11: Orbit with constant eccentricity ε=0.75. Left: Position of inner cylinder. Right: plot of the pressure [bar] at mid cylinder. The last picture shows the line where the pressure was sampled. Radius of Orbit $R_O=3.75\cdot10^{-5}$ m, Cycle Duration T=0.015 s.

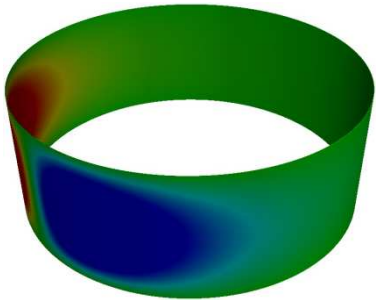

FIG.12: Orbit with constant eccentricity ε=0.75. 3D pressure distribution (red-blue corresponds high-low pressure)

First, one should discuss the existence of negative pressure. It is a well known problem of the Reynolds equation, a two- dimensional approximated Navier- Stokes equation for the bearing. The code solves the given equations for the problem. Behind the smallest gap there theoretically can be calculated negative pressure (*FIG.13*). The oil in the gap is incompressible and can take very high pressure. But it is not possible to reduce it to any desired value, because a fluid cannot transmit tractive forces. The fluid will evaporate if a critical low pressure is reached. So later in the project there we will be used a two phase solver that fulfils this point. But nevertheless the Reynolds equation predicts quite well the regions where critical pressure may occur in a simple bearing.

And so do this three- dimensional solver. The final question would be how to connect this pressure with a probability of cavitation. That point will be investigated in a later stage of the project. *FIG.13* shows the different pressure distributions in a bearing. Sommerfeld was the first who analytically solved the Reynolds equation (1904). Gümbel (1921) introduced the boundary condition to put all negative pressure to zero. This method was very successful for basic calculations of a bearing and was in well agreement to his experiments. Reynolds demanded a smooth solution.

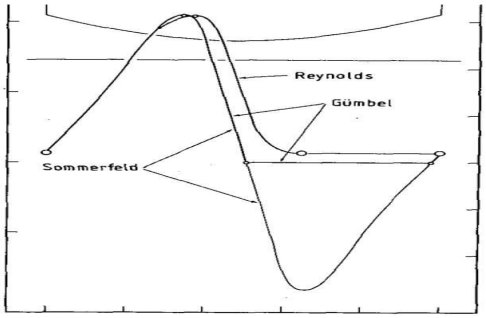

FIG.13: Pressure distribution in a bearing in circumferential direction: Sommerfeld (negative pressure), Gümbel (heavy discontinuity, sets every negative pressure to zero) and Reynolds demanded smooth function [2]

The pressure distribution of all 10 post processing positions shows that the low pressure region is behind the smallest gap. This is the place where cavitation may occur. Because of the constant eccentricity there is no change in the location of the minima and maxima. They just move along with the smallest gap.

4.2. Orbit with oscillating eccentricity

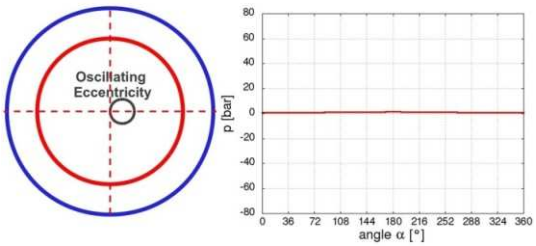

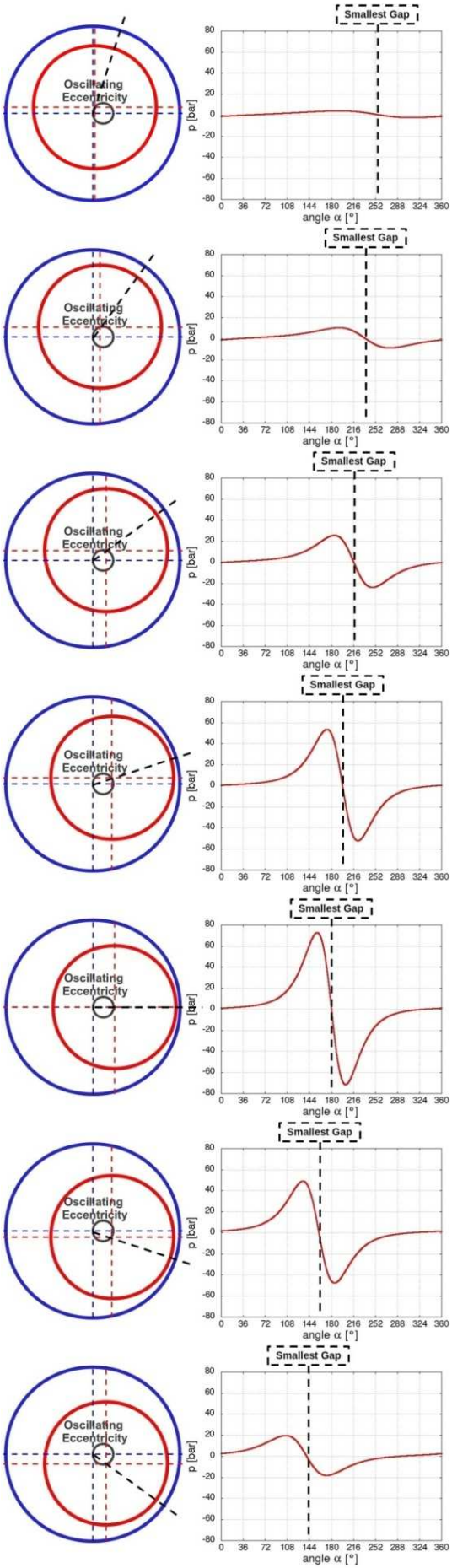

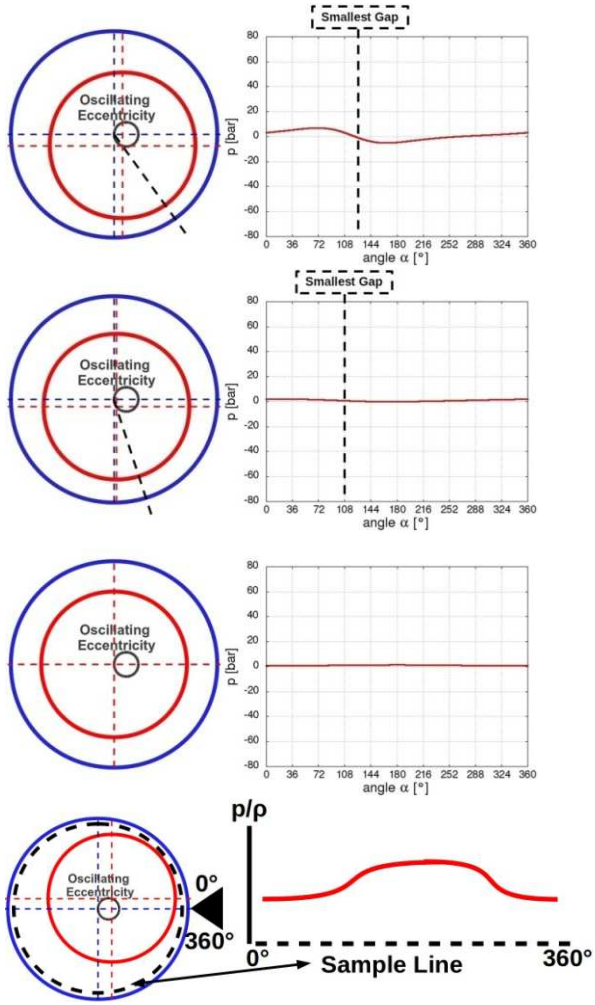

FIG.14: Orbit with oscillating eccentricity. Simulation starts concentric. After the half of the orbit the system reaches ε =0.75. Then the inner rotating cylinder moves back to the concentric position. Left: Position of inner cylinder. Right: plot of the pressure [bar] at mid cylinder. The last picture shows the line where the pressure was sampled. Radius of Orbit: $R_O=1.87\cdot10^{-5}$ m, Cycle Duration: T=0.015 s.

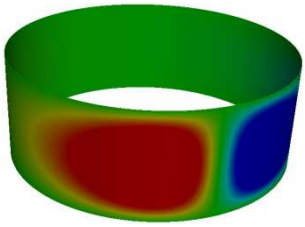

FIG.15: Orbit with oscillating eccentricity. Simulation starts concentric. 3D pressure distribution (red-blue corresponds high-low pressure). This picture shows the system at its maximum eccentricity ε =0.75.

In case of oscillating eccentricity the orbit starts from the concentric position. There is no narrowing or expanding gap where low or high pressure regions can develop. Then the eccentricity rises. The pressure in front of the smallest gap increases the same as it decreases behind the smallest gap. So the pressure gradients grow until the maximum of eccentricity is reached after the half of the orbit. Now the eccentricity diminishes again and the pressure gradients break down. So the results are in well agreement to the two-dimensional results.

5. Outlook

We designed a simplified three-dimensional bearing model with implemented offset track of the inner rotating shaft. For first tests we chose an orbit as crankshaft offset track. The code was successfully tested for onset and decay of TV. Furthermore it is possible to implement other offset tracks.
The model can predict critical regions for the pressure for a given offset track of the inner rotating cylinder. At the moment we run simulations with implemented cavitation model to compare the predicted pressure regions with cavitation probabilities for the same cases with Ψ=1‰. The main goal is to investigate the effect of different geometries on cavitation probabilities. The next step will be the simulation of more detailed geometries with implemented oil feedings and notches.

References:

[1]: C. Daniel, J. Strackeljan, E. Woschke, Modellierung von Gleitlagern in rotordynamischen Modellen, Conference on Vibrations in Rotating Machines (SIRM), 2009

[2]: N. Hannoschöck, Kolbenringschmierung und Verschleiß, Dissertation ETH 7635

[3]: H. Jasak, Z. Tukovic, Automatic Mesh Motion for the Unstructured Finite Volume Method, 2004

[4] G. Knoll, K. Backhaus, J. Lang, K. Wilhelm, Berechnungen von Motoren-gleitlagern unter Berücksichtigung der Deformation, www.ist-aachen.com/tower1.pdf, 1995

[5]: B. Künne, Köhler/Rögnitz Maschinenteile 2, Vieweg & Teubner, 10.Auflage, ISBN: 3835100920, 2008

[6]: P. Moradnia, Project work for the PhD course in OpenFOAM, A tutorial on how to use Dynamic Mesh solver IcoDyMFOAM, 2008

[7] M. Schmidt, Numerical meshing issues for three-dimensional flow simulation in journal bearings, 3rd Micro and Nano Flows Conference

[8] N. Herzog, P. Stücke, C. Egbers, Numerical and experimental study of the flow in an eccentric Couette-Taylor system with small gap, PAMM, Vol. 8, Issue 1, pp 10641–10642, 2008

[9] L. S. Siong, An Experimental Investigation Of Taylor- Couette Flow Between Eccentric Cylinders, Master Thesis, National University of Singapore, 2006

[10] J. H. Spurk, N. Aksel, Einführung in die Theorie von Strömungen, Strömungslehre (6. Auflage), Springer, Berlin Heidelberg, ISBN: 3-540-26293-8, 2006

[11] P. Stücke, N. Herzog, C. Egbers, Numerische Simulation der Strömung in Gleitlagern, PAMM Vol. 5, Issue 1, pp. 555–556, 2005

[12] P. Stücke, M. Nobis, M. Schmidt, 3D-Flow Structures in Journal Bearings, SAE Power trains Fuels and Lubricants, SAE International, 2009

[13] http://www.enginehistory.org/Piston/Rotax912/06a_rotax912_crankshaft_original.JPG

[14]: http://www.openfoam.com/features/standard-solvers.php